

NEAR-INFRARED IMAGING POLARIMETRY OF THE GG TAU CIRCUMBINARY RING¹

JOEL SILBER,² TIM GLEDHILL,² GASPARD DUCHÈNE,³ AND FRANÇOIS MÉNARD⁴

Received 3 March 2000; Accepted 9 May 2000

ABSTRACT

We present 1 micron *Hubble Space Telescope*/NICMOS resolved imaging polarimetry of the GG Tau circumbinary ring. We find that the ring displays east-west asymmetries in surface brightness as well as several pronounced irregularities, but is smoother than suggested by ground-based adaptive optics observations. The data are consistent with a 37° system inclination and a projected rotational axis at a position angle of 7° east of north, determined from millimeter imaging. The ring is strongly polarized, up to $\sim 50\%$, which is indicative of Rayleigh-like scattering from sub-micron dust grains. Although the polarization pattern is broadly centrosymmetric and clearly results from illumination of the ring by the central stars, departures from true centrosymmetry and the irregular flux suggest that binary illumination, scattering through unresolved circumstellar disks, and shading by these disks, may all be factors influencing the observed morphology. We confirm a $\sim 0''.25$ shift between the inner edges of the NIR and millimeter images and find that the global morphology of the ring and the polarimetry provide strong evidence for a geometrically thick ring. A simple Monte Carlo scattering simulation is presented which reproduces these features and supports the thick ring hypothesis. We cannot confirm filamentary streaming from the binary to the ring, also observed in the ground-based images, although it is possible that there is material inside the dynamically cleared region which might contribute to filamentary deconvolution artifacts. Finally, we find a faint 5th point source in the GG Tau field which, if it is associated with the system, is almost certainly a brown dwarf.

Subject headings: stars: individual: GG Tau – stars: pre-main-sequence – binaries: close – polarization – scattering

1. INTRODUCTION

GG Tau is one of the most studied systems known to possess a tidally truncated circumbinary disk. It is a double binary, in which all four components display evidence of infrared excesses (White et al. 1999) indicating the presence of unresolved circumstellar disks. However, the most striking object in the system is the large disk of gas and dust surrounding the northern ($\sim 0''.25$) binary.

Since the circumbinary structure was first detected (Beckwith et al. 1990; Simon & Guilloteau 1992; Kawabe et al. 1993), many of its physical parameters have been constrained, particularly from the millimeter interferometry of Dutrey, Guilloteau, & Simon (1994) and Guilloteau, Dutrey, & Simon (1999, hereafter GDS). The disk is tidally truncated by the dynamical action of the binary at a radius of $\sim 180\text{AU}$ from the binary center of mass and extends out to at least 800AU. From their most recent millimeter continuum and CO line flux measurements, GDS propose that 90% of the dust component of the circumbinary disk lies in a well-defined *ring* (inner radius $\sim 180\text{AU}$; outer radius $\sim 260\text{AU}$) within the extended (800AU) disk. Their observations are consistent with an almost circular Keplerian disk, rotating about the binary's center of mass with a projected rotational axis at a position angle (PA) of 7° east of north, and viewed at an inclination of 37° to face-on. This implies that the northern part of the ring is closest to us (the 'front') and that the southern part of the ring corresponds to the 'back'.

The first near-infrared (NIR) observations of the ring

were obtained with ground-based adaptive optics (AO) by Roddier et al. (1996, hereafter RRNGJ) who published deconvolved *J*, *H*, and *K* band images of the ring. Their data show a very clumpy ring and suggest a large degree of anisotropy in its illumination. The images also show radial filaments *inside* the dynamically cleared cavity, extending from the binary to ring. At the *J* and *K* bands, the ring appears incomplete (or at least *very* faint) at the back. GDS found that when they registered their 1.4mm and RRNGJ's *J* band image, there is a $\sim 0''.25$ shift of the ring's NIR inner edge towards the binary. This could be explained if the dust ring is *geometrically thick*, extending to a height of $\sim 120\text{AU}$ at its tidally truncated inner radius.

In this paper, we present the first resolved imaging polarimetry of the GG Tau system and the first space-based images of the circumbinary ring. We refer to the northern binary as 'GG Tau' and follow GDS in assuming a distance of 140AU to the Taurus star-forming region (Elias 1978).

2. OBSERVATIONS AND DATA REDUCTION

Imaging linear polarimetry data of GG Tau were obtained on 1998 April 3 with the Near Infrared Camera and Multi Object Spectrometer (NICMOS) on the *Hubble Space Telescope* (*HST*) (Proposal 7827). Camera 1 (NIC1) was used to image GG Tau through the three polaroid filters, POL0S, POL120S, and POL240S, of central wavelength $1.0459\mu\text{m}$ ($1\mu\text{m}$) at a pixel scale of $0''.043$. The detector was operated in MULTIACCUM mode enabling

¹Based on observations made with the NASA/ESA *Hubble Space Telescope*, obtained at the Space Telescope Science Institute, which is operated by AURA, Inc., under NASA contract NAS5-26555.

²Department of Physical Sciences, University of Hertfordshire, Hatfield, Hertfordshire, AL10 9AB, U.K.

³Laboratoire d'Astrophysique, Observatoire de Grenoble, Université Joseph Fourier, B.P. 53, 38041 Grenoble Cedex 9, France

⁴Canada-France-Hawaii Telescope Corporation, PO Box 1597, Kamuela, HI 96743

multiple non-destructive read-out of the array during integration. Our data were re-reduced using the STSDAS package NICPROTO to remove the ‘pedestal’ and ‘shading’ image anomalies (Dickinson et al. 1999). We calculated the Stokes parameters and associated errors from our data using an IDL implementation of the algorithm developed by Sparks & Axon (1999) and the polaroid coefficients of Hines (1998).

A PSF subtraction or deconvolution is essential to reveal the faint circumbinary material surrounding GG Tau, since the PSF wings from the binary are highly extended and possess diffraction spikes which fill the entire frame. We have used our own observations of the DF Tau *binary* to subtract the GG Tau PSFs. DF Tau is the closest binary in our sample and its $\sim 0''.1$ separation is at the *HST*/NICMOS resolution limit. The relative flux and absolute location of the GG Tau and DF Tau components were measured with iterative PSF fitting in DAOPHOT (Stetson 1987). We then created a ‘double’ image for each GG Tau polaroid by shifting and adding the original image to itself with the relative flux and separation of the DF Tau components. Appropriately scaled DF Tau PSFs were then subtracted from these new images. We are confident that the total flux subtracted is correct to within the photometric errors, and that the PSF registration is accurate since the diffraction spikes are subtracted to almost undetectable levels away from the PSF cores.

3. RING MORPHOLOGY

A one micron PSF-subtracted NIC1 image of GG Tau is presented in Figure 1(a). Although there are subtraction residuals in the stellar cores and diffraction spikes, the ring is exceptionally well revealed. Unlike the smooth continuum flux distribution at 1.4mm (GDS), and like RRNGJ’s *J* and *H* band images, the ring shows an unambiguous north-south asymmetry. A relatively thin bright arc of scattered light from the northern (front) part of the ring dominates the image with broader and fainter flux from the south (back) completing what is, essentially, an unbroken ring. The ring appears far less clumpy than in RRNGJ’s images.

The ring exhibits several examples of irregular structure: (i) the arc is brighter on its east side; (ii) there is a ‘kink’ in the ring’s south-east portion; (iii) there is a possible gap/dimming of the ring (unfortunately) at the location of the western diffraction spike. Although GDS determined the large-scale distribution of dust to be quite smooth, they used a $0''.9 \times 0''.6$ beam, and it is possible that the irregularities we observe may be due to small-scale inhomogeneities in the ring. However, it is more likely that we are witnessing the effects of anisotropic illumination of the ring from the binary light sources and shading by the stars’ circumstellar disks. There is some evidence of scattering from clumps of dusty material *inside* the dynamically cleared region at the locations of *both* of RRNGJ’s *J* and *H* band filamentary streamers. However, these clumps lie close to the subtraction residuals in our image and may be residuals in their own right. If real, it is possible that RRNGJ’s filaments are deconvolution artifacts caused by actual material inside the ring.

We have overlaid several ellipses on to our image in Figure 1(b) to help clarify the ring geometry. These have been located at the center of mass of the binary, assuming a 1:1 mass ratio. Ellipses 1 and 2 (green) represent circles of radii 180AU ($1''.29$) and 260AU ($1''.86$), viewed at

an inclination of 37° to face on, and should be interpreted as the projected millimeter (GDS) bounds of the ring *in its equatorial plane*. Ellipse 3 (cyan) marks the projected ring/cavity boundary based on GDS’s ring inclination, inner edge radius, and estimate of inner edge ring thickness (§1). Scattered light is clearly observed inside ellipse 1, both at the front and the back of the ring whereas we find that ellipse 3 provides a good bound to the scattered flux edges, particularly at the front of the ring. Thus we are able to confirm the $\sim 0''.25$ displacement of the NIR front edge inwards towards the binary with respect to the 180AU inner edge derived from 1.4mm continuum imaging. This is consistent with scattering occurring high up in a geometrically thick ring, away from its equatorial plane. Further evidence for this comes from the morphology of front and back scattered flux. Figure 2 demonstrates how an optically and geometrically thick ring will produce the scattered flux morphology of the observations – the narrower flux at the front and broader flux at the back. In contrast, a geometrically thin ring would produce similar widths of scattered flux from the front and back of the ring, and an optically thin ring would produce homogeneous flux similar to GDS’s 1.4mm continuum image. Knowledge of the ring’s orientation allows us to deduce that the thin bright arc must be caused by forward-scattering off the ring’s upper front surface and the broad fainter flux results from back-scattering off the rear upper surface and ring inner edge.

Following Close et al. (1998), who re-examined the RRNGJ images, we measured the ratio of total flux received from the front and back parts of the ring. Use of RRNGJ’s ‘ring zone’ (concentric ellipses with semi-major axes $1''.25$ and $1''.90$) and rotational axis PA (20° east of north) does not make sense with our image. Instead, the ratio was measured for all flux lying outside of our ring inner bound, ellipse 3. We obtain a value of 1.17 ± 0.06 which is considerably less than that measured by Close et al. (1998) from RRNGJ’s *J* band image (3.6 ± 1.0). We have also measured the azimuthal *intensity* profile of flux contained within two (non-concentric) ellipses, namely ellipse 3 and an additional ellipse $0''.3$ larger than ellipse 3 in both semi-axes (not shown). These measurements reveal a maximum flux intensity ratio of ~ 4.0 between the peak of the brighter side of the arc and the back of the ring. This contrasts with the $>10:1$ (2.8 magnitudes difference) obtained by RRNGJ from their deconvolved *J* band data. This measurement provides an additional constraint for modelling the system.

4. RING POLARIZATION

We present in Figure 1(c) the first resolved linear polarization map of the GG Tau ring. At 1 micron the ring displays a broadly centrosymmetric scattering pattern which clearly indicates illumination of the ring by the central stars. A detailed interpretation of the polarization pattern will require inclusion of binary sources and, probably, the effect of the binary’s circumstellar disks. The high polarization levels observed at 1 micron, up to $\sim 50\%$, are indicative of Rayleigh-like scattering from sub-micron particles. The polarization is at a minimum ($\sim 20\%$) in the bright arc at the front of the ring and a maximum ($\sim 50\%$) in the broad region at the sides and back. Using the geometry proposed by GDS, the scattering angles involved are typically $\sim 35^\circ$ at the front and $\sim 109^\circ$ (or greater) at the back (Figure 2). Maximum polarization in the Rayleigh

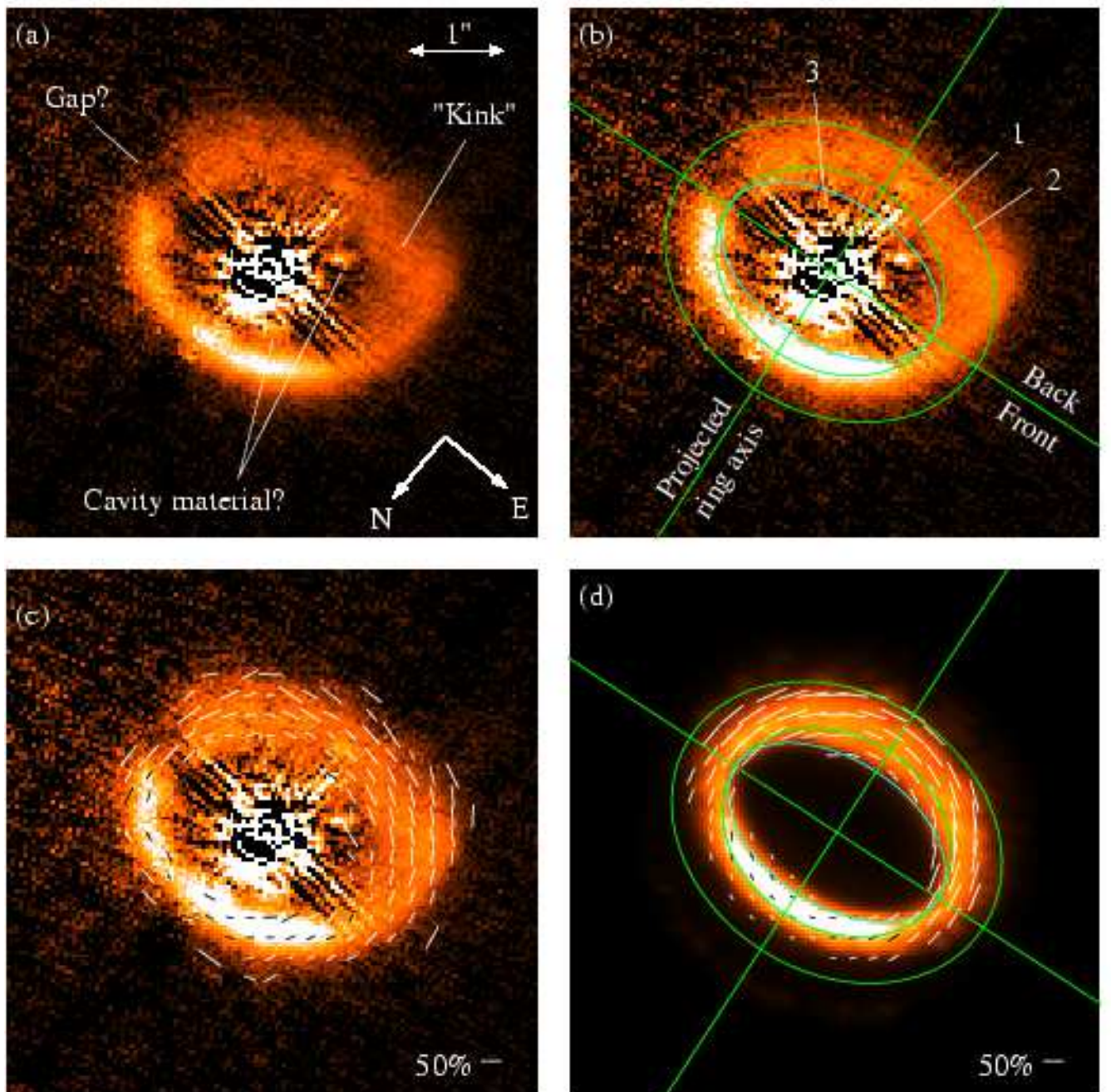


FIG. 1.— *Left:* NIC1 PSF subtracted image of GG Tau at 1 micron revealing the circumbinary ring. Subtraction residuals, most obvious in the core and inner diffraction spikes remain due to the low sampling of the PSF image and errors in the relative separation and flux of the GG Tau and DF Tau binaries. The image is $5''6$ on a side ≈ 800 AU assuming a distance of 140 parsec to Taurus (Elias 1978) and has been scaled linearly to reveal irregularities and asymmetries. *(b)* and *(c)*: The same data overlaid with the projected rotational axis of the ring and ellipses based on the geometric findings of Guilloteau et al. (1999), and with linear polarization vectors. These images have been rescaled to highlight the northern bright arc. *(d)*: a simple Monte Carlo scattering simulation of the ring, overlaid with polarization vectors.

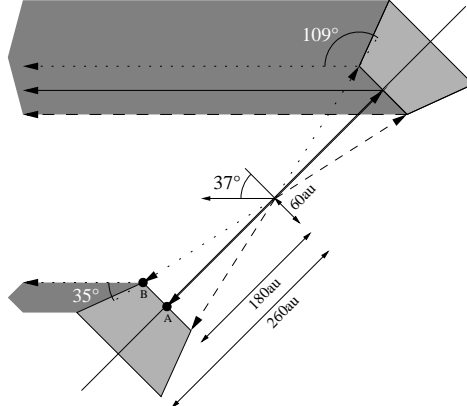


FIG. 2.— A representation of the thick ring geometry proposed by Guilloteau et al. (1999). Several light paths are drawn for single-scattering off the inner edges and surface of the *optically* thick ring. The different projected surface areas from which scattered light is visible to an observer on the left result in very different thicknesses of observed flux around the ring (dark shading). This is exactly what is seen in our 1 micron image. This effect is reduced as one moves to thinner ring geometries (reduction of the disk height A→B). In addition, this geometry predicts lower levels of polarization at the front of the ring than the back for Rayleigh-like scattering, since the scattering angles at the back (109°) are closer to the maximum polarization scattering angle (90°) than those at the front (35°). This is also observed in the data.

regime occurs when photons are scattered through right-angles and, consequently, since the back is scattering 36° closer to maximum polarization than the front, it is more highly polarized. Thus our polarimetry observations are entirely consistent with a thick disk geometry (§1). This behaviour would not be observed with a thin disc where front and back scattering angles are equally close to 90°.

5. SIMPLE MODEL

We performed some simple, single source, Monte Carlo multiple scattering simulations to try and reproduce the ring's major morphological and polarization features with a thick disk geometry. We did not attempt any detailed calibration to previous determinations of disk/ring mass, but sought only to demonstrate the effects of a geometrically and optically thick ring on the scattering and polarization patterns. The ring was modelled as an arbitrary standard flared disk ($\alpha = 2$ and $\beta = 1.05$) with Gaussian truncated inner and outer edges (parameters used by GDS). The dust density distribution parameters were all free, so there is bound to be much degeneracy between absolute density, scale height, flaring parameter β , and radial density power law α .

Our best simulation is presented in Figure 1(d) and has been overlaid with its corresponding polarization vectors. Following Close et al. (1998), who implicitly modelled the ring as a flat structure, we used the Mathis & Whiffen (1989) dust grain model 'A' with a steeper grain size power law ($p = -4.7$). However, this simulation retained the model's original maximum grain size of $0.9\mu\text{m}$. The major features of the observations are all reproduced with an integrated front/back flux ratio of 1.0 and front/back maximum intensity ratio of 3.3 fitting the data well. The shift inwards of the inner edge of the ring of $0''.25$, noted by GDS, is reproduced and is roughly consistent with their ring thickness estimate at the inner edge of 120AU at a radius of 180AU. The global polarization features (low at the front, high elsewhere) are reproduced with polarization levels ranging from 10% to 80%, values broadly within our errors. This is another powerful endorsement of the geo-

metrically thick disk hypothesis.

More thorough modelling of the ring will be the subject of a future paper which will consider scattering through, and shading by, the unresolved circumstellar disks, the effect of binary sources, and choice of dust grain model, all of which will affect the scattering and polarization patterns. Finding the correct grain model is vital if the ring is to be modelled successfully, as this determines both the front/back flux ratios and the levels of polarization. Further observations of GG Tau are essential and, in particular, only multiple wavelength resolved polarimetry of the ring will provide enough constraints on the grain model to remove this as a free parameter.

6. A FIFTH ELEMENT?

We note the presence of a fifth point source in the GG Tau field which is considerably fainter than the possibly substellar (White et al. 1999) secondary of the *southern* binary. It is located off the field of Figure 1, $6''.16$ ($\sim 860\text{AU}$) from the primary of the northern binary at a PA of 242° east of north. Although the source appears in the previously published coronagraphic images of Nakajima & Golimowski (1995), these authors make no reference to it and we can find no comment regarding the object in the literature. We note that GG Tau does not lie in the densest region of the Taurus-Auriga star-forming complex and the object may well be a background star. However, if it does lie at the same distance as GG Tau then, given its faintness, it is almost certainly a brown dwarf.

We wish to thank Dave Axon and Bill Sparks for early access to preprints and their IDL polarimetry code, Eddie Bergeron for assistance with image re-reduction, John Krist for advice on the PSF subtractions, and Phil Lucas and Hiro Takami for assistance with the Monte Carlo simulations. We acknowledge use of the data analysis facilities provided by the Starlink Project which is run by CCLRC on behalf of PPARC. An anonymous referee is thanked for useful comments.

REFERENCES

- Beckwith, S. V. W., Sargent, A. I., Chini, R. S., & Güsten, R., 1990, *AJ*, 99, 924
- Close, L. M., et al., 1998, *ApJ*, 499, 883
- Dickinson, M., et al., 1999, NICMOS Data Handbook Version 4.0, Space Telescope Science Institute
- Dutrey, A., Guilloteau, S., & Simon, M., 1994, *A&A*, 286, 149
- Elias, J. H., 1978, *ApJ*, 224, 857
- Guilloteau, S., Dutrey, A., & Simon, M., 1999, *A&A*, 348, 570 (GDS)
- Hines, D. C., 1998, in ESO Conference and Workshop Proceedings 55, NICMOS and the VLT: A New Era of High Resolution Near Infrared Imaging and Spectroscopy, ed. W. Freudling & R. Hook (Garching: ESO), 63
- Kawabe, R., Ishiguro, M., Omodaka, T., Kitamura, Y., & Miyama, S. M., 1993, *ApJ*, 404, L63
- Mathis, J. S., & Whiffen, G., 1989, *ApJ*, 341, 808
- Nakajima, T., & Golimowski, D. A., *AJ*, 109, 1181
- Roddier, C., Roddier, F., Northcott, M. J., Graves, J. E., & Jim, K., 1996, *ApJ*, 463, 326 (RRNGJ)
- Simon, M., & Guilloteau, S., 1992, *ApJ*, 397, L47
- Sparks, W. B., & Axon, D. J., 1999, *PASP*, 111, 1298
- Stetson, P. B., 1987, *PASP*, 99, 191
- White, R. J., Ghez, A. M., Reid, I. N., & Schultz, G., 1999, *ApJ*, 520, 811